NASA CONTRACTOR REPORT 166302

Carbon Fibers Conductivity Studies

Cary Y. Yang and
Aldona M. Butkus

CONTRACT NAS2-10188
August 1980

NASA

NASA CONTRACTOR REPORT 166302

Carbon Fibers Conductivity Studies

Cary Y. Yang
Aldona M. Butkus
Surface Analytic Research, Inc.
1662 Parkhills Avenue
Los Altos, California 94022

Prepared for
Ames Research Center
under Contract NAS2-10188

National Aeronautics and
Space Administration

Ames Research Center
Moffett Field, California 94035

This Page Intentionally Left Blank

TABLE OF CONTENTS

INTRODUCTION

The high tensile strength and light weight characteristics of carbon fiber composites have attracted industrial attention as potential replacement for heavier metal materials used in space and ground vehicles. However, due to their high electrical conductivity, inadvertent release of the carbon fibers can pose fire hazards by interfering with unprotected electrical contacts. In order to attempt to alleviate potential danger from carbon fibers and yet to preserve their properties as light weight, high strength material, a basic understanding of the process of electrical conduction in carbon fibers and how it is affected by structural variations became desirable. Two approaches were used in this study. One focused on the role residual nitrogen played in fiber conductivity while the other addressed the feasibility of fiber modification to achieve electrical conductivity reduction. The first approach supplemented the work by Rabii, et al[1] on electronic energy band calculation for graphite with substitutional hetero atoms. The second approach complemented the band structure calculations of Fong and Tsang[2] on oxygen intercalated graphite.

When polyacrylonitrile (PAN) is subjected to oxidation and subsequent heat treatment, most of the non-carbon elements are driven off and the polymer chains condense forming aromatic hexagonal networks of carbon atoms. The resultant carbon fiber possesses enormous stiffness and strength as well as electrical conductivity several orders of magnitude greater than that of the starting material. Recent elemental analysis of PAN samples carbonized between 650-900°C[3] indicate substantial nitrogen retention. Based on 1) the nitrogen content results, 2) electrical conductivity as a function of heat-

treatment temperature (HTT),[4] 3) fiber mean crystallite dimensions,[5,6] and 4) an idealized scheme previously proposed[7,8] for the carbonization of PAN fibers (Figure 1 of Appendix I), nitrogen site models of PAN fibers at low HTT were studied.

Calculations were carried out on cluster models of PAN fiber consisting of carbon, nitrogen, and hydrogen atoms using the modified intermediate neglect of differential overlap (MINDO) molecular orbital (MO) method.[9] The models were developed based on the assumption that PAN fibers with HTT below 1000°C retain nitrogen in a graphite-like lattice. The clusters studied are shown in Figure 2 of Appendix I. For clusters modeling an "edge" nitrogen site (Appendix I, Figure 2, clusters a,b,c) analysis of the occupied MO's indicated an electron distribution similar to that of graphite. A similar analysis for the somewhat less stable "interior"nitrogen site (Figure 2, cluster d) revealed a partially localized π electron distribution around the nitrogen atom. A summary of the electron distributions is presented in Figure 3 of Appendix I. The calculated binding energies for the clusters are reported in Table II of Appendix I.

Differences in bonding trends and structural stability between edge and interior nitrogen cluster calculations modeling PAN fiber led to the following conclusions. If an interior nitrogen model is adopted in order to explain the high nitrogen content in low HTT PAN fiber, loss of nitrogen from interior sites is predicted to take place preferential to nitrogen loss from edge sites. No significant change in stiffness or crystallite size is expected with this interior nitrogen loss. However, this process could be at least partly responsible for the

observed dramatic conductivity variation[4] in the HTT range of 600-1000°C. At HTT above 1000°C the conductivity increase is leveling off[4] and the nitrogen to carbon atomic ratio could be more readily explained by the presence of only edge nitrogens.. A more detailed explanation of the effects of residual nitrogen loss in PAN fibers is presented in Appendices I and II.

The second part of the carbon fiber study dealing with possible fiber modification considered the possible electrical conductivity reduction by intercalation as modeled by oxygen intercalated graphite. This idealized model was chosen based on the observation of extensive graphitic domains present in high HTT PAN fibers. Oxygen was chosen as the intercalant since it could form strong bonds with carbon and thus tying up the conduction electrons. Electrical conductivity reduction would then be expected.

For the oxygen intercalation study, cluster calculations were again carried out using the MINDO approach. The graphite models consisted of both a full three dimensional representation as well as an independent layer model of the lattice. Four different positions were chosen for the oxygen atom and are indicated in Figures 1,2,3,4 of Appendix III. The oxygen-graphite layer distances in the cluster models were optimized within a rigid lattice approximation. This results in the oxygen atom being the most energetically favored at a distance of 1.25 Å above a carbon-carbon bond. Additionally, oxygen interaction with the carbons of only one graphite plane predominated. A more detailed account of the calculations as well as a summary of the results can be found in Appendix III. Evidence of strong oxygen-carbon bonding suggested

strong interaction with the graphite conduction electrons, hence leading to an insulating phase.

The calculations that have been performed dealing with the carbon fiber electrical conductivity problem represent the first attempt in interpreting, elucidating, and predicting properties in carbon fibers using a localized cluster model approach. In view of the general lack of long-range order in PAN carbon fibers a less extended picture is necessary than that provided by band structure calculations and cluster models can help establish general bonding trends and local electronic charge transfers and binding strengths. Coordination of such theoretical approaches with experimental efforts are essential in attaining a better understanding of PAN fibers and hence a better control over their properties.

REFERENCES

1. S. Rabii, R. Tatar, and D. DiVincenzo, University of Pennsylvania. Work performed under NASA Ames contract.

2. C.Y. Fong and Y. Tsang, University of California, Davis. Work performed under NASA Ames contract.

3. D.E. Cagliostro, Textile Research Journal, in press.

4. T. Yamaguchi, Carbon 2, 95 (1964).

5. J.B. Donnet, A. Voet, H. Daukoch, P. Ehrburger, and P. Marsh, Carbon 11, 430 (1973); ibid 431 (1973).

6. W.N. Reynolds, in Chemistry and Physics of Carbon, Vol. 11, Dekker, New York, 1973, p.1

7. P.J. Goodhew, A.J. Clarke, and J.E. Bailey, Materials Science and Engineering 17, 3 (1975).

8. G.M. Jenkins and K. Kawamura, "Polymeric Carbons," Cambridge University Press, Cambridge (1976) pp. 90-105.

9. R.C. Bingham, M.J.S. Dewar and D.H. Lo, J. Amer. Chem. Soc. 97, 1302 (1975).

Appendix I

ELECTRONIC STRUCTURE OF CLUSTERS MODELING PAN CARBON FIBERS

Aldona M. Butkus and Cary Y. Yang

Surface Analytic Research, Inc.
1662 Parkhills Avenue
Los Altos, CA 94022

A B S T R A C T

In an attempt to understand the process of electrical conduction in polyacrylonitrile (PAN)-based carbon fibers, calculations were carried out on cluster models of the fiber consisting of carbon, nitrogen and hydrogen atoms using the modified intermediate neglect of differential overlap (MINDO) molecular orbital (MO) method. The models were developed based on the assumption that PAN carbon fibers obtained with heat treatment temperatures (HTT) below 1000°C retain nitrogen in a graphite-like lattice. For clusters modeling an "edge" nitrogen site, analysis of the occupied MO's indicated an electron distribution similar to that of graphite. A similar analysis for the somewhat less stable "interior" nitrogen site revealed a partially localized π electron distribution around the nitrogen atom. The differences in bonding trends and structural stability between edge and interior nitrogen clusters led to a two-step process proposed for nitrogen evolution with increasing HTT.

I. INTRODUCTION

When polyacrylonitrile (PAN), $(CH_2\text{-}CH(CN))_n$ where n is typically 2000 in commercial fibers, is subjected to oxidation and subsequent heat treatment, most of the non-carbon elements are driven off and the polymer chains condense forming aromatic hexagonal networks of carbon atoms. The resultant carbon fiber possesses enormous stiffness and strength as well as electrical conductivity several orders of magnitude greater than that of the starting material. Electron microscopy and x-ray diffraction studies[1] of these carbon fibers indicate that each fiber consists of ribbons of crystallites bundled together and cross-linked, while being aligned along the fiber axis. The typical crystal structure within each ribbon is that of turbostratic graphite possessing no regular stacking order in the direction perpendicular to the basal plane. Since PAN carbon fibers are non-graphitizable, the interplanar spacing, while decreasing with increasing heat treatment temperature (HTT), never reaches that of pure graphite even at the highest HTTs. Values of L_a and L_c, the mean crystallite dimensions parallel and perpendicular to the basal planes, increase with increasing HTT. For PAN carbon fibers with HTT around 1000°C, values of about 20Å for the width L_a and about 10Å for the thickness L_c are typical.[1,2]

Recent elemental analysis of PAN samples carbonized between 650-900°C indicated substantial nitrogen retention[3], the nitrogen to carbon atomic ratio ranging from 0.24 to 0.15. An idealized scheme showing the nitrogen sites previously proposed[4,5] for the carbonization process of PAN fiber is indicated in Figure 1. Assuming the ribbon models shown in Figure 1 as possible intermediate structures during the

carbonization process, we have calculated the nitrogen to carbon ratio with increasing ribbon width, L_a, and the results are given in Table I. This model allows the presence of only "edge" nitrogens. In order to accomodate the high percentage of nitrogen in the samples reported in Reference 3, L_a have to be between 10 and 15Å in that range of HTT. However, the crystallite dimensions of these samples are not available. Since extensive graphitized domains exist in PAN carbon fibers with HTT below 1100 C[1], such small widths seem unlikely. Hence the retained nitrogen probably resides in additional sites. Discounting the presence of interstitial nitrogens, one is left with the only alternative, namely, the substitution of an interior carbon in the two-dimensional graphite environment by a nitrogen atom. This substitution is similar to that in heterocyclic compounds with bridgehead nitrogen atoms, e.g. cycl [3.3.3] azines. However, the only chemical evidence for the existence of a stable interior nitrogen during the carbonization process is the large amount of nitrogen at low HTT. The effects on structure and electrical conductivity of the presence of such an interior nitrogen in contrast to an edge nitrogen constitute the main thrust of this work. The role of other mechanisms such as hydrogen loss or contribution from impurity levels[5,6] giving rise to changes in electrical conductivity during the carbonization process of carbon fibers has not been addressed.

II. METHOD OF CALCULATION

In order to study the structural stability and general bonding trend of nitrogen substitution in PAN carbon fibers, modified intermediate neglect of differential overlap (MINDO/3)[7] molecular orbital calculations have been carried out on clusters of atoms consisting of carbon, nitrogen and hydrogen modeling the nitrogen site environment. The MINDO/3 approach was chosen because it allows one to obtain the ground state solution to the electronic Schrodinger equation for polyatomic systems in considerably less computation time. This savings over the ab initio Hartree-Fock-Roothaan molecular orbital approach is achieved through either the neglect or the replacement by parameters of certain Hartree-Fock Hamiltonian matrix elements. These parameters have been previously determined through a lengthy iterative procedure by fitting experimental geometries and heats of formation for a large class of molecules[8]. Additionally, since it is of interest in the present study to determine possible changes in geometry with the introduction of nitrogen into the graphite lattice, total energy minimization as a function of atomic coordinates would be desirable and could be economically performed with the MINDO/3 approximation.

The clusters chosen to model the nitrogen sites in the fiber are shown in Figure 2. A few calculations were carried out on three dimensional cluster models of the nitrogen site assuming an ideal graphite stacking geometry. But since these three dimensional studies yielded results identical to those of the two dimensional models and the interlayer

structure of the fiber is basically turbostratic, with no long range order in the direction perpendicular to the basal plane, the ensuing analysis will be based on the two dimensional models. In order to minimize edge effects introduced by a finite cluster representation of the lattice, hydrogen atoms were used to saturate the valence of the outer carbons. Geometry optimizations were carried out and the heats of formation were obtained. Study of the effect of nitrogen substitution on conductivity was based on the calculated electron distribution in orbitals perpendicular to the basal plane (π electrons). This was accomplished using a Mulliken population analysis[9], which is a means of partitioning electron density among the various atoms in the cluster from the calculated molecular orbitals.

Previously, theoretical study of the one-ring and three-ring structures had been carried out. The single ring calculation[10] was performed with MINDO/3, which is also employed here. But since the Mulliken population analysis was not reported[10], we have repeated the one-ring calculation. The earlier study of the three-ring structures was done using a more approximate semi-empirical approach with only the π orbitals determined self-consistently[11].

III. RESULTS AND DISCUSSION

Geometry optimization of the various cluster models shown in Figure 2 yields planar environments about the nitrogen for both the interior and the edge nitrogen models. The carbon-nitrogen bond length for the edge nitrogen model varies from 1.335Å (single-ring model) to 1.356Å (four-ring model), while a carbon-nitrogen bond length of 1.416Å is obtained for the interior nitrogen case. The carbon-hydrogen distances are all approximately 1.10Å, a value typically found in aromatic molecules. Differences in geometry between the various edge nitrogen models are within 2% indicating that any structural changes due to the presence of nitrogen are local to the substitution site and do not significantly affect the adjacent rings.

Analysis of the occupied molecular orbitals for the edge nitrogen models shows that as in the pure graphite case one electron from each ring atom (carbon or nitrogen) is present in the π -type orbitals perpendicular to the basal plane, with the remaining electrons participating in σ -bonding with the adjacent in-plane carbons. The non-bonding lone pair orbital on nitrogen normal to the edge surface then becomes the analog of the third σ bond of the pure graphite case.

For the interior nitrogen site, three σ -type bonds are formed with the adjacent carbons in the basal plane similar to those in graphite, the carbon-nitrogen bond distance being very close to that of carbon-carbon in graphite. However, the remaining two valence electrons,

being partially localized on nitrogen, are donated to the π system, resulting in a very different π electron distribution from that of graphite. In order to better see these changes in the π system, the fractional π electron charge at each atom is calculated by dividing the electron population in the orbital perpendicular to the basal plane (p_π) by the total atomic population for the particular atom. A summary of the calculated values is given in Figure 3. This fractional π charge at each atom is used instead of the explicit p_π population because the former approach better represents the actual σ-π breakdown for all atoms, regardless of their environment.

In order to investigate the relative stability of the nitrogen in the two sites, the average binding energy per atom relative to atomization is calculated for an edge nitrogen model (4-ring), an interior model (3-ring), as well as a pure graphite model analogous to the edge model. The results are summarized in Table II for the three cases.

From the fractional π electron distribution shown in Figure 3, it becomes apparent that the edge nitrogen gives rise to a more even electron distribution than the interior nitrogen case. In fact, the former resembles pure graphite in its π electron distribution. As with the geometry optimization results, effects due to the presence of an edge nitrogen are confined to the nearest carbon neighbors. In contrast, the π electron distribution for the interior nitrogen site

shows a significant variation as one passes from atom to atom. Since it is the electrons in the π system that are responsible for the conductivity along the basal plane, the partial localization of the electrons would imply a reduction in conductivity for the fiber with an interior nitrogen. On the other hand, the edge nitrogen would not be expected to play as large a role in changing the conductivity.

The relative stability of the two sites as estimated from the average binding energies yields an energy difference of approximately 0.25eV (5.8 kcals/mole) between the edge and interior models indicating that the edge site is energetically favored over the interior one. This energy difference is remarkably close to the experimentally determined value of 5.9 kcals/mole for the barrier to inversion for ammonia. The transition state for this process requires the atoms to be coplanar, placing a steric constraint on the nitrogen similar to that present in the interior nitrogen model.

Thus if an interior nitrogen model is adopted in order to explain the high nitrogen content in low HTT PAN fiber, loss of nitrogen from interior sites is predicted to take place preferential to nitrogen loss from the edge sites. No significant change in stiffness or crystallite size is expected with this interior nitrogen loss. However, we propose that this process is at least partly responsible for the observed dramatic conductivity variation[12] with heat treatment of PAN fibers in the temperature range of 600-1000°C. If one adopts the two-

dimensional graphite touching band picture[13], the partial localization of π electrons most likely results in a somewhat flattening of the valence and conduction bands. According to semiconductor band theory, the consequences of such band flattening are generally two-fold. First, the band gap opens up; and second, the carrier effective masses increase. One would also expect that nitrogen in the graphite lattice, whether or not in an ordered arrangement, will shorten the carrier life-times through increased charge localization. Hence, the overall effect of nitrogen retention on the electrical properties of PAN carbon fibers is a decrease in the conductivity resulting from simultaneous decreases in carrier densities and mobilities. In view of the more localized π electrons around the <u>interior</u> nitrogen atom, we believe that nitrogen retention in the interior provides one important physical mechanism responsible for the drastic decrease in conductivity of PAN carbon fibers up to 1000°C HTT.

At HTT above 1000°C the conductivity increase is leveling off[12] and values for L_a (20-30Å) and the nitrogen to carbon atomic ratio[14] (0.09) can now be readily accounted for by the presence of <u>only</u> edge nitrogens. The results reported here do not indicate a direct effect on the conductivity due to the loss of edge nitrogen. However, it can be inferred from the large concentration of electron density about the edge nitrogen atom (due to the protruding lone pair) that coalescence of the ribbons to form a larger hexagonal carbon net would be inhibited based on electrostatic grounds. With the loss of these edge nitrogens

leading to coalescence and hence larger crystallite dimensions, the carrier mobility due to ribbon boundary scattering will increase. Since in this range of HTT, the resistivity is probably dominated by scattering from ribbon boundaries[15], and since larger crystallite dimensions give rise to greater π delocalization as well as extended σ linkage, increases in conductivity and stiffness would result. This proposed two-step nitrogen elimination could also help explain the observed sharp increase in nitrogen evolution[16] around 900°C, since at this temperature nitrogen loss from both sites could be occurring simultaneously.

IV. CONCLUSIONS

The calculations presented here represent the first attempt in interpreting and elucidating properties in carbon fibers using a localized cluster model approach. Previous attempts [17,18] have been based on information directly derived from an assumed band structure. It is our contention that a less extended picture is necessary to provide complementary data whereby properties of the material can be better understood. In view of the general lack of long-range order in PAN carbon fibers, cluster models can help establish general bonding trends such as those found in the nitrogen-containing clusters.

Our suggestion that the π bands are flattened due to nitrogen retention will hopefully be verified by the ongoing calculations of Rabii[19] on nitrogen graphite. From the band structure, we hope to estimate the conductivity as a function of nitrogen concentration, i.e. HTT. The two-step nitrogen elimination model proposed here should stimulate more measurements of the crystallite dimensions of low HTT PAN carbon fibers, as well as more spectroscopy experiments. We believe that systematic experimental and theoretical efforts, properly coordinated, are essential in attaining a better understanding of PAN carbon fibers, and hence a better control over their properties.

ACKNOWLEDGEMENTS

This work is supported by the National Aeronautics and Space Administration Ames Research Center under Contract NAS2-10188. The authors thank D. E. Cagliostro, C. F. Hansen, N. R. Lerner, J. A. Parker, S. Rabii, and T. E. Thompson for valuable discussions.

REFERENCES

1. J.B. Donnet, A. Voet, H. Dauksch, P. Ehrburger, and P. Marsh, Carbon 11, 430 (1973); ibid., 431 (1973).

2. W.N. Reynolds, in Chemistry and Physics of Carbon, Vol. 11, Dekker, New York, 1973, p. 1.

3. D.E. Cagliostro, Textile Research Journal, in press.

4. P.J. Goodhew, A.J. Clarke and J.E. Bailey, Materials Science and Engineering 17, 3 (1975).

5. G.M. Jenkins and K. Kawamura, "Polymeric Carbons". Cambridge University Press, Cambridge (1976), pp. 90-105.

6. N.R. Lerner, J. Polym. Sci., Phys. Ed., (submitted).

7. MINDO/3 program from National Resource for Computational Chemistry, Lawrence Berkeley Laboratory, Berkeley, CA.

8. R.C. Bingham, M.J.S. Dewar, D.H. Lo, J. Amer. Chem. Soc. 97, 1285 (1975).

9. R.S. Mulliken, J. Chem. Phys. 23, 1833 (1955).

10. R.C. Bingham, M.J.S. Dewar, and D.H. Lo, J. Amer. Chem. Soc. 97, 1302 (1975).

11. M.J.S. Dewar and N. Trinajastic, J. Chem Soc. (A), 1754 (1969).

12. T. Yamaguchi, Carbon 2, 95 (1964).

13. For a review of graphite band structure, see I.L. Spain, in "Chemistry and Physics of Carbon," Vol. 8, eds. P.L. Walker and P.A. Thrower, Marcel Dekker, New York (1973).

14. A.K. Fiedler, E. Fitzer, and F. Rozploch, Carbon 11, 426 (1973).

15. A.A. Bright and L.S. Singer, Carbon 17, 59 (1979).

16. W. Watt, Nature, 236, 10 (1972).

17. S. Mrozowski, Carbon 9, 97 (1971).

18. K. Yazawa, J. Phys. Soc. Japan 26, 1407 (1969).

19. S. Rabii, presented in this conference.

TABLE I. Nitrogen to carbon atomic ratio and number of interior rings as a function of approximate ribbon width L_a for ribbon model of PAN fiber carbonization process.

L_a(Å)	Ratio N to C	Number interior rings
7	0.33	1
9	0.25	2
11	0.20	3
13	0.17	4
15	0.14	5
20	0.11	7
30	0.07	12

TABLE II. Average binding energy per atom for the nitrogen edge (4-ring) and interior (3-ring) models and the four-ring cluster graphite model.

Cluster	Energy (eV/atom)
N-edge	5.28
N-interior	5.03
Graphite	5.22

FIGURE CAPTIONS

Figure 1. The development of graphite structures during the pyrolysis of thermally stabilized PAN.

Figure 2. Cluster models chosen for edge (a,b,c) and interior (d) nitrogen sites in PAN fiber.

Figure 3. Fractional π electron polulation for (a) edge nitrogen model, (b) interior nitrogen model, and (c) graphite model.

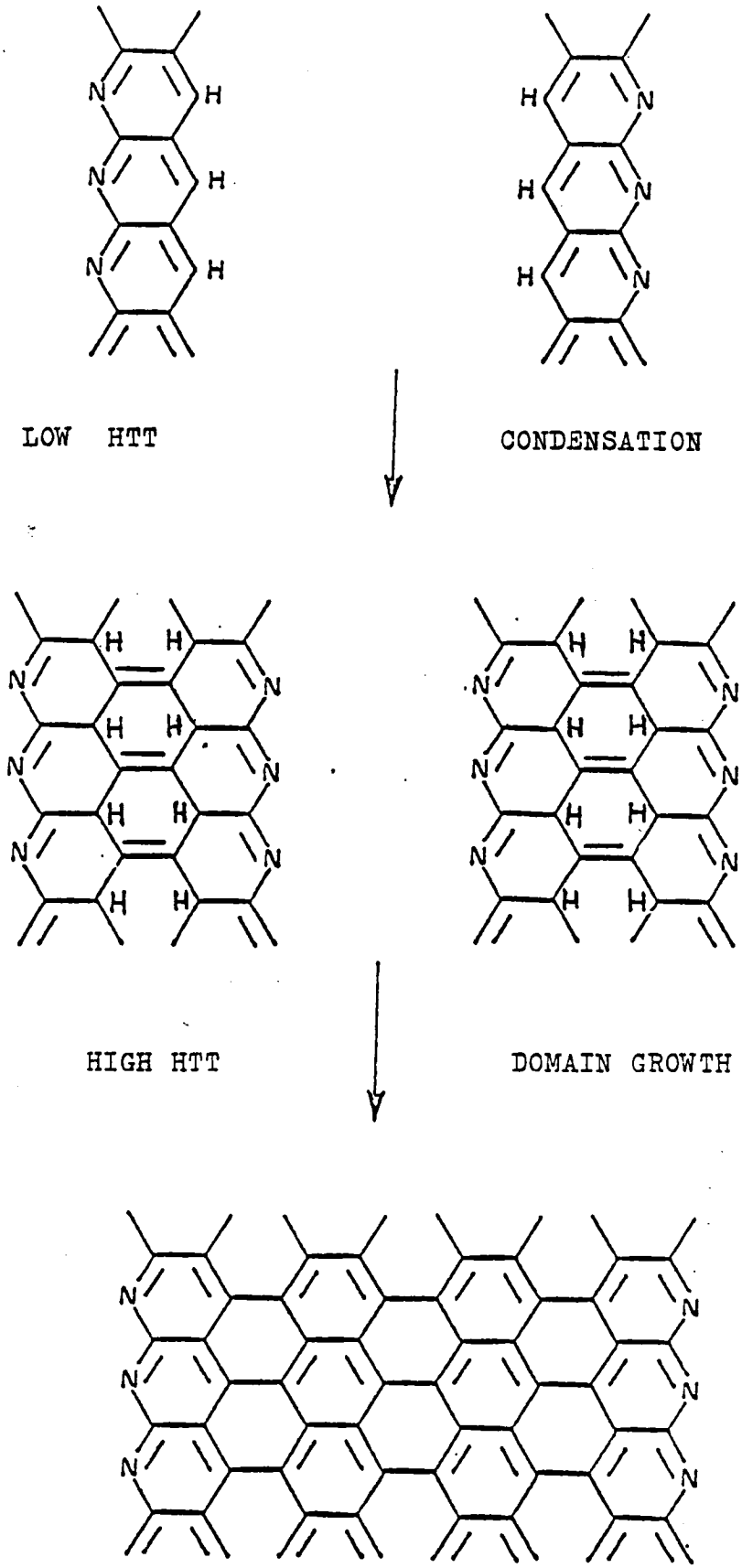

Figure 1

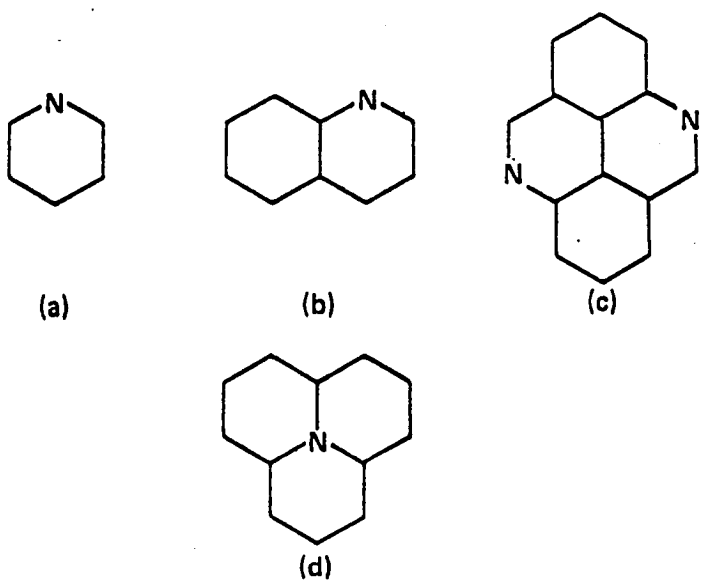

Figure 2

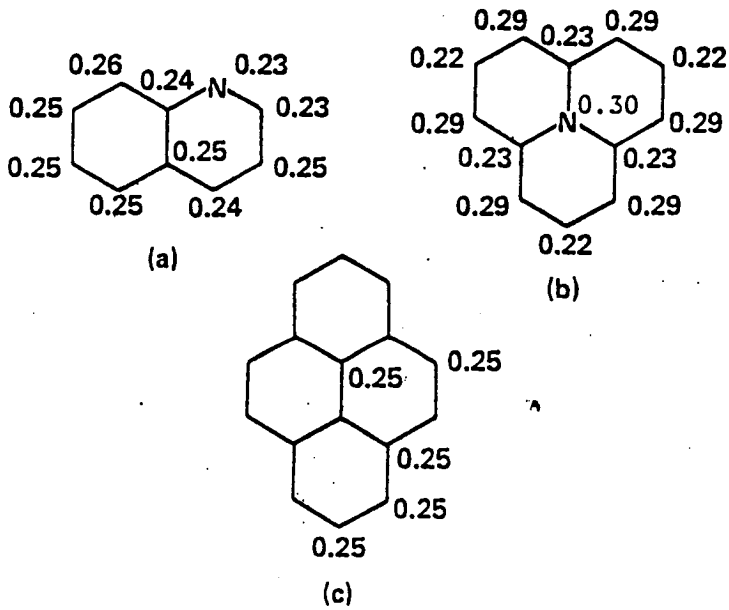
0.26
0.24
N
0.23
0.25
0.23
0.25
0.25
0.25
0.25
0.24
(a)
0.29
0.23
0.29
0.22
0.22
0.30
N
0.29
0.29
0.23
0.23
0.29
0.29
0.22
(b)
0.25
0.25
0.25
0.25
0.25
(c)

Figure 3

Appendix II - To be submitted to Synthetic Metals

Properties and Modelling of PAN-Based Carbon Fibers

Thomas E. Thompson

SRI International, Menlo Park, CA 94025

Cary Y. Yang

Surface Analytic Research, Inc., Los Altos, CA 94022

C. Frederick Hansen

NASA Ames Research Center, Moffett Field, CA 94035

Summary

A review of the properties of PAN-based carbon fibers is presented with a view toward developing a meaningful model for theoretical calculations and the analysis of experimental data. After reviewing the status of past and present models, the results of the first cluster calculations of the electronic structure of carbon fibers is presented.

1. Introduction

There has recently been increased interest in the electrical properties of carbon fibers. Much of this interest stems from the highly desirable mechanical properties of these fibers (four times stronger than steel and only one-quarter the density) which leads to their use as strength-giving elements in plastic composite materials. Current applications of carbon-fiber composites range from tennis rackets to the bay doors on NASA's space shuttle. The possibility of making strong light-weight cables and other electrical applications provides strong impetus to the materials engineer and solid-state scientist to understand the nature of the electronic conduction mechanism in carbon fibers and the relationships between the conductivity, the structure, and the mechanical properties of the fibers, all of which are related to properties of the precursor material and the processing history.

The room-temperature electrical conductivities of commercial carbon fibers range from 500 - 5000 $(\Omega\text{-cm})^{-1}$. These values are considerably lower than the basal-plane conductivity of pristing graphite or copper, which have values of 25,000 and 580,000 $(\Omega\text{-cm})^{-1}$, respectively; however, certain chemical treatments of carbon fibers have been shown to increase the fiber conductivity by an order of magnitude [1 - 4], into a range with more engineering potential. The fact that this increase can only be produced with fibers which have been processed in a certain manner gives further reason to study the basic electrical properties of carbon fibers.

In this paper we first present a review of the properties of carbon fibers with a view toward developing a meaningful model for theoretical calculations

and the analysis of experimental data, we then discuss the status of past and present models and present the results of cluster calculations which provide the first theoretical picture of the electronic structure of carbon fibers. For the sake of brevity and in order to develop a specific model, we have chosen to concentrate on carbon fibers made from precursor fibers of polyacrylonitrile (PAN). PAN-based carbon fibers are presently used for most composite applications, having replaced the rayon-based carbon fibers which were developed a decade ago. Pitch-based fibers, which are still in the developmental stage, are the third type of carbon fiber of significant commercial interest. Even though we concentrate on the PAN-based fiber many aspects of the discussion will apply to carbon fibers from other precursors, as will be pointed out.

2. Properties of PAN-Based Carbon Fibers

2.1 Production, Chemistry, and Mechanical Properties

The homopolymer polyacrylonitrile (PAN) upon which the carbon fiber is largely based, has the formula $[CH_2\text{-}CH(CN)]_n$, where the degree of polymerization, n, for commercial fibers is usually higher than 2000. Commercial PAN fibers such as DuPont's "Orlon" also contain copolymers such as vinyl acetate, vinyl chloride, or styrene to improve such properties as their ability to stretch or their affinities for dyes, and the precursor materials for commercial carbon fibers also contain a number of additives [5].

Commercial carbon fibers are produced from PAN fibers by first "oxidizing" the PAN fiber under tension at a temperature near 250°C, then carbonizing and heat treating in an inert atmosphere at temperatures from 1200 to 3000°C.

Figure 1 shows some possible intermediate structures during these production steps as conceived by Watt [6]. The lower temperature "oxidation" drives off hydrogen, possibly produced ketonic groups (-CO-), and causes a cross-linking of CN groups to produce a ladder structure. Tension is applied to assure alignment of these ladders along the fiber axis, a necessary condition for the production of high modulus fibers. This alignment is preserved with the final heat treatment even if the tension is removed. Between the 250°C "oxidation" and the subsequent high temperatures treatments various amounts of water, HCN, N_2, CO, CO_2 and other gases are given off and the ladder chains evolve into an aromatic hexagonal network of carbon atoms. Figure 2, from Fiedler, et al. [7] shows typical data for the rate of gas evolution for PAN fibers as various heat treatment temperatures (HTT). Fibers produced with HTTs near 1500°C typically have from 5 to 16 percent non-carbon residue. The exact structure of the carbon sheets is not known and the way that the residue fits into the actual atomic structure of the fiber has not yet been clearly determined. One of the goals of our research is to gain an understanding of this structure through a correlation of experimental results with theoretical models.

The processing HTT can be directly correlated with the resulting mechanical properties of the fibers as shown by the data of Watt and Johnson [8], presented in Figure 3. The modulus of PAN-based carbon fibers rises continuously with HTT, however, the tensile strength passes through a maximum value near 1500°C and then decreases with increasing HTT. Because of this maximum, commercial PAN-based carbon fibers are available either with high tensile strengths and medium stiffness moduli, or high moduli and medium strengths. The former group includes such fibers as Union Carbide's Thornel 300, manufactured by Toray in Japan; Celanese's Celion 6000, from Japan by Toho-Beslon;

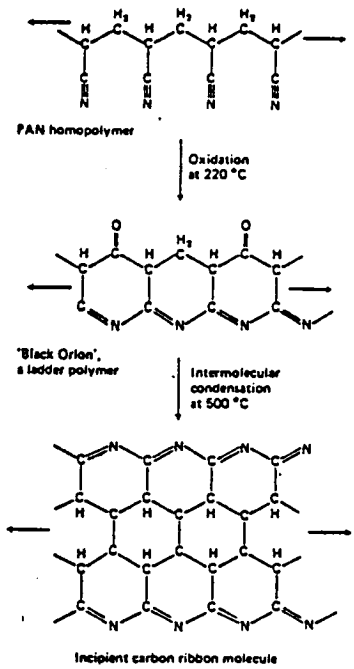

Figure 1. The chemical changes which occur as PAN fibers are turned into carbon fiber as described by Watt, Ref. 6.

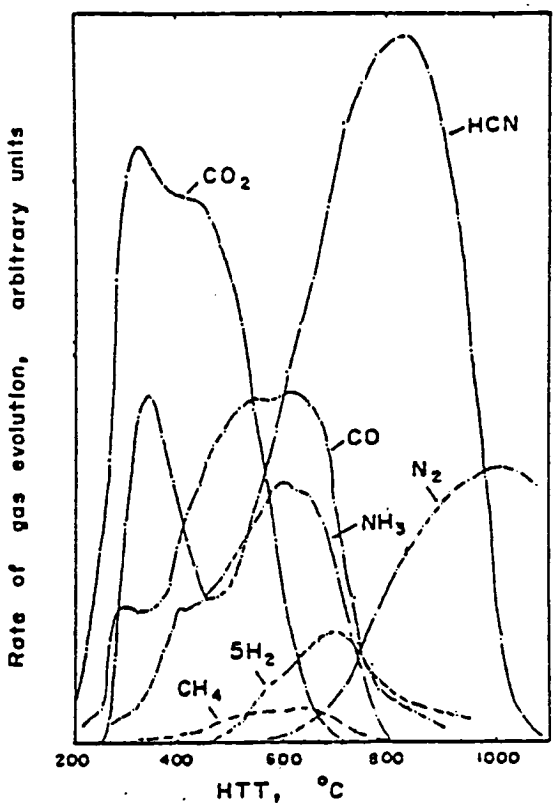

Figure 2 The evolution of gases during the heat treatment of PAN fibers, from Ref. 7.

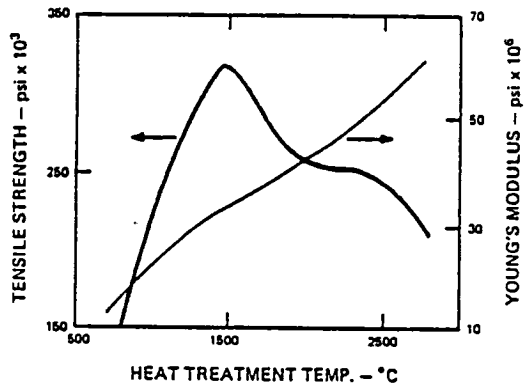

Figure 3 The HTT dependence of tensile strength and Young's modulus for PAN-based carbon fibers, from Ref. 8.

and Hercules' HTS2 until recently produced in England by Courtaulds. An example of a high modulus fiber is Celanese's GY70. Table 1 summarizes typical values for moduli and tensile strengths and their relationships with the HTT along with several other properties of PAN-based carbon fibers and the properties of graphite. Whereas PAN-based carbon fibers cannot be transformed into graphite it is interesting to see how the density, modulus, and resistivity of the fibers approach those of graphite as the HTT is increased. This relationship will be discussed further in subsequent sections.

2.2 Structure

Typical of the models of the structure of PAN-based fibers is that presented by Wicks [9], shown in Figure 4, in which a fiber consists of bundles of microfibrils that lie along the fiber axis. In this model, the result of numerous x-ray and electron diffraction studies, each fibril is made up of parallel layers of hexagonally-arrayed carbon atoms. The layers are "turbostratic", i.e. randomly stacked, and lack the three-dimensional order of graphite as indicated by the absence of certain (hkl) x-ray reflections. The details of the structure of each fibril, as well as the alignment of the fibrils, depend upon the HTT and the stress conditions during production. For example, the separation between the carbon sheets varies from 3.4 to 3.7 angstroms [10], with the closest spacing for PAN fibers reached only with heat treatment above 2000°C. However, even at the highest treatment temperatures the ideal graphite spacing, 3.35 angstroms, cannot be attained. This is another way of saying that PAN fibers are non-graphitizable as we mentioned earlier. Fibril thicknesses, L_c, vary from 30 to 100 angstroms, with a characteristic straight section, L_a, of the order of 100 angstroms, again, depending on the heat treatment history. A typical set of data for L_c and L_a from Johnson and Tyson [11] is plotted in Figure 5.

MATERIAL	HEAT TREATMENT TEMPERATURE	PERCENTAGE CARBON	DENSITY (G/CM^3)	TENSILE STRENGTH (10^3 PSI)	YOUNG'S MODULUS (10^6 PSI)	RESISTIVITY ($\mu\Omega$ - CM)
CARBON FIBERS FROM PAN	~1500°C	92%	1.7	400	32	1500
	$\gtrsim$2200°C	99	2.0	250	75	700
PYROLITIC GRAPHITE (BASAL PLANE)	>3000°C	99+	2.2	2800	148	40

TABLE 1 TYPICAL PROPERTIES OF PAN/CARBON FIBERS WITH DIFFERENT HEAT TREATMENT TEMPERATURES COMPARED WITH PYROLYTIC GRAPHITE

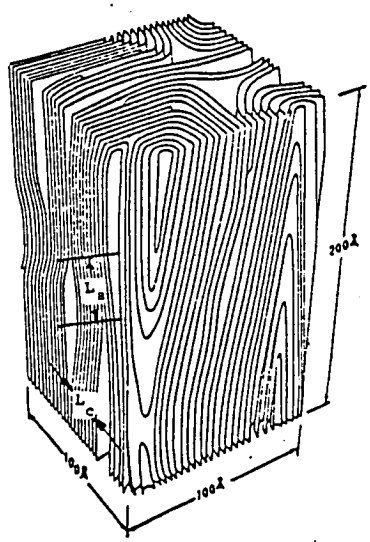

Figure 4 Schematic three-dimensional model of the carbon fiber structure, from Ref. 9.

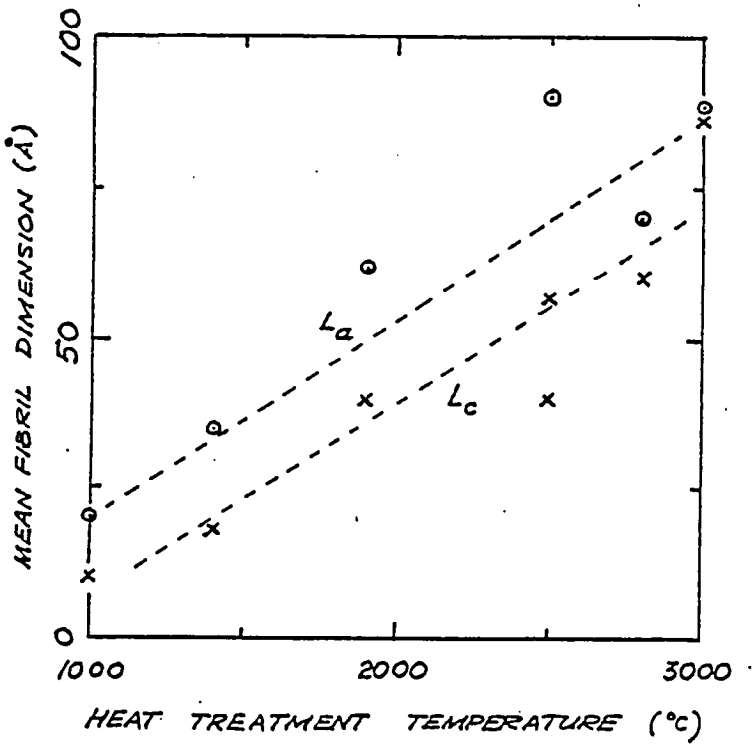

Figure 5 The HTT dependence of the fibril dimensions, data from Ref. 11.

In Figure 4, needle-shaped voids can be seen. These voids, which are mostly inaccessible to helium, can represent from 5 to 30 percent of the total volume. The fibers also contain impurities and residuals from the precursor materials, e.g., the high strength, medium-modulus PAN-based carbon fibers are only 90 percent carbon, as mentioned earlier.

Recently, several heterogeneous structures have been proposed for PAN-based carbon fibers, such as a core with a radial structure of crystalline webs separated by large voids and the core surrounded by a highly crystalline sheath [12]. However, Bennett and Johnson [13] have shown that these fibers have a rather homogeneous structure not unlike that depicted in Figure 4. Only with heat treatment at 2500°C is the sheath/core heterogeniety observed and then the sheath is thin, from 100 to 1500 angstroms.

The modulus and strength of carbon fibers is basically derived from the covalent bonds between the hexagonally-arrayed carbon atoms within each sheet. These are the same bonds which give graphite a basal-plane modulus or 150 X 10^6 psi. The planar covalent bonds, called σ - bonds, are sp^2 hybrid orbitals involving three of the four valence electrons of each carbon atom. They are actually stronger than the sp^3 bonding orbitals of diamond. In order for these bonds to be effective the sheets of carbon atoms must be parallel to the fiber axis. This is achieved by stretching the fiber during the initial oxidation assuring that the ladder chains are aligned along the fiber axis.

2.3 Electrical Properties

The relationship between the HTT and the electrical properties of PAN-based carbon fibers was first published by Yamaguchi in 1963 [14]. His results and

a comparison with soft carbons are shown in Figure 6. The dramatic decrease in the resistivity above 600°C parallels the onset of the planar-sp^2 (or σ) bonding which eventually leads to the turbostratic structure which we have previously discussed. This relationship between bonding and electrical conduction was clearly shown by Ezekial in 1970 [15] when he comapred the resistivity and Young's modulus for both rayon-based and PAN-based carbon fibers. Ezekial's results are shown in Figure 7 which also includes data points from Table 1. The information from Figures 6 and 7 leads us to picture the increased conduction as arising from the formation of π - bands which accompany the formation of the strength-giving σ bonds. Pristine graphite, the ideal crystalline material toward which the fibers tend, is a semimetal with electron and hole concentrations of $n = p \sim 10^{19}$ cm^{-3}, each with mobilities near 10^4 $cm^2/V{\cdot}s$, resulting in a room-temperature resistivity of $\rho = 4 \times 10^{-5}$ Ω-cm. The minimum resistivity for the fibers shown in Figure 6 is approximately twenty times that value.

At two recent meetings the first comprehensive data was presented on the temperature dependence of electrical conductivity of PAN-based carbon fibers. Kalnin and Goldberg [4] gave data for five different sets of PAN-based fibers, all of which had been teat treated above 2000°C and had moduli between 50×10^6 and 110×10^6 psi. Gillespie, Ehrlich, and Waters [3] presented $\rho(T)$ curves for the commercial fibers AS, HMS, T-300, and GY-70 as well as two pitch fibers. Between 50 and 300 K all of the resistivity curves show a monotonic decrease in resistivity with increasing temperature similar in slope and magnitude to the data resistivity taken by Bright and Singer [16] for pitch-based carbon fibers, which is given in Figure 8. The data for the AS and T-300 fibers, which have HTTs near 1500°C, have the extra feature that ρ peaks near 25K with a 4 percent decrease in ρ between 25K and 4K. The decrease in

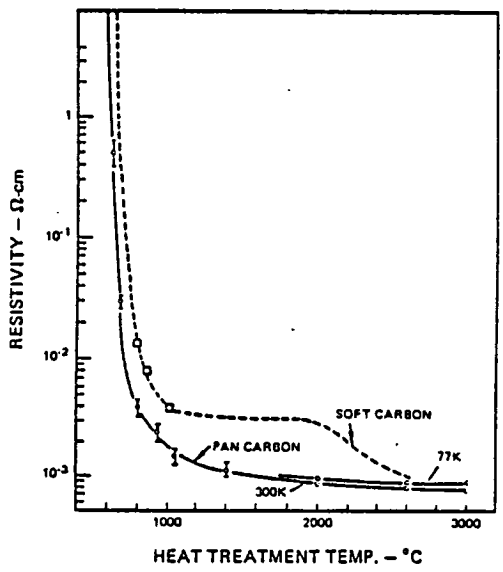

Figure 6 Carbon resistivity as a function of HTT, from Ref. 14

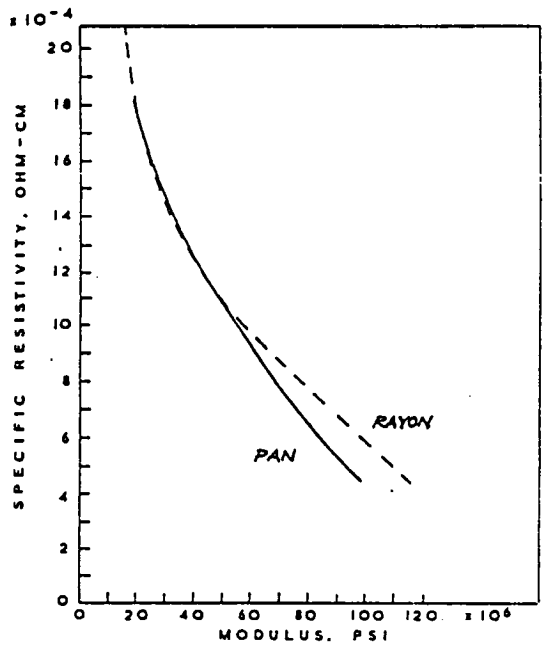

Figure 7. The relationship between resistivity and modulus for two types of carbon fibers, from Ref. 15.

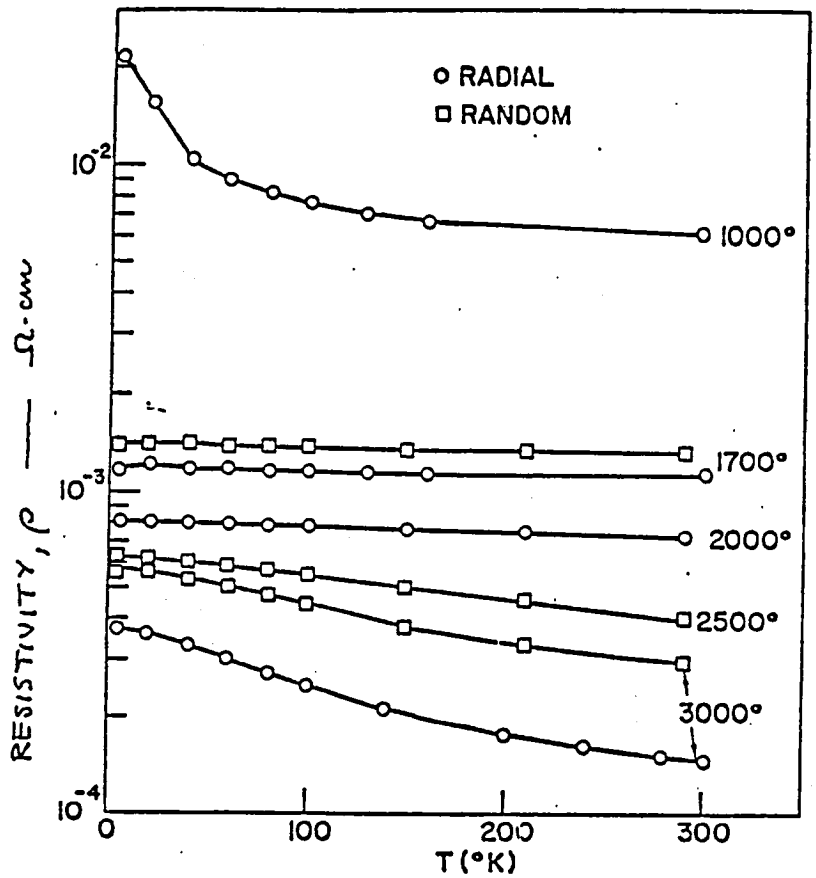

Figure 8 Resistivity as a function of temperature for pitch-based carbon fibers, from Ref. 16.

resistivity with increasing T most likely indicates that the charge carriers in the fibers are thermally activated as in a semiconductor or semimetal with shallow overlap of bands. A similar temperature dependence was noted by Hérinckx for rayon-based carbon fibers [17]. The only other published resistivity data for PAN-based carbon fibers is that of Robson et al. [18], shown in Figure 9, where the resistivity ratio between liquid nitrogen and room temperature is given as a function of HTT. There is an interesting similarity between the data in Figures 8 and 9: they both have a minimum in the resistivity ratio near HTT 1750°C.

The magnetoresistance effect has proven to be a useful analytical tool in semiconductors because its magnitude is related to the mobilities of the carriers. Unfortunately, the interpretation of the magnetoresistance in carbon fibers and pyrocarbons can be complicated by a negative contribution which is still not understood even though it has been studied extensively [19, 20]. Robson et al. [18] showd that the negative effect arises in PAN/carbon fibers which have HTTs greater than 1750°C, as shown in Figure 10. This is a property that will have to be addressed in future models of these materials.

3. Models

Akamatu and Inokuchi [21] showed that compounds with carbon-ring structures exhibited conductivities with semiconductor-like temperature dependences even for as few as nine rings, and Mrozowski [22] extended this idea to explain the experimental results on soft carbons. He proposed a variable-band-gap model in which successively higher heat treatment of soft carbon change them from semiconductors to semimetals, with the band gap decreasing to zero and then into an overlap region. In Mrozowski's model the carbon atoms begin to form

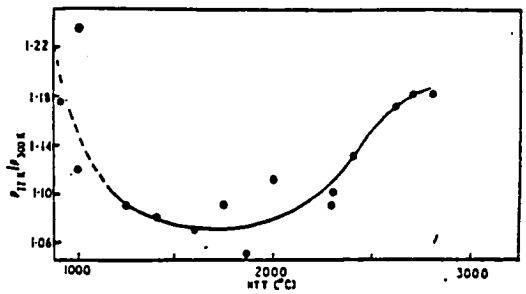

Figure 9 The HTT dependence of the resistivity ratio for PAN-based fibers, from Ref. 18.

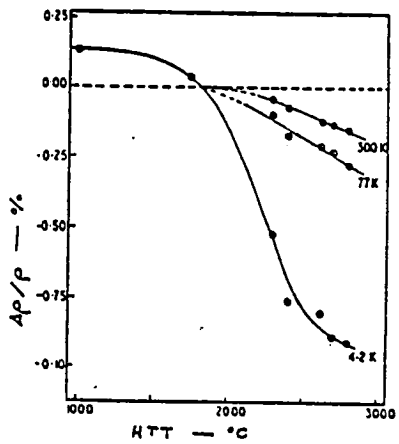

Figure 10 The magnetoresistance for PAN-based carbon fibers as a function of HTT, from Ref. 18.

an aromatic structure upon heat treatment near 600°C, with the π electrons forming valence and conduction band with an energy gap of ~ 0.3 eV. With higher heat treatment the gap decreases, going to zero near 1200°C, as the lamellar carbon planes become larger and the spacing between the turbostratically aligned layers decreases. With heat treatment above 3000°C the carbons assume the three-dimensional ordering of graphite, where the bands overlay by approximately 0.04 eV.

Over the years, a number of models have been proposed for carbon fibers in attempts to explain and elucidate various structural and electronic properties. Yazawa [23], for example, employed a two-dimensional band model of graphite with adjustable parameters and successfully predicted the variation of magnetoresistance and Hall coefficient with HTT, magnetic field and sample orientation. Both models are based on the energy band picture of a crystalline solid. In view of the general lack of long-range order, even for high HTT carbon fibers, a less extended picture for the material needs to be developed, not necessarily as an independent verification of the band models, but rather to complement them. It was in this spirit that calculations were initiated in 1979 by Butkus and Yang on the electronic structure of model clusters of PAN carbon fibers, and by Rabii on the band structure of nitrogen graphite.

The cluster calculations of Butkus and Yang [24] have been performed using a combination of two semi-empirical quantum chemical methods, MINDO/3 and HAM/3. The object of these calculations is to examine the localized bonding picutre in nitrogen-retained PAN carbon fibers. Previously, we have established that regions of turbostratic graphite do exist within PAN-based carbon fibers at low HTT's. This gives rise to the underlying assumption that PAN-based carbon fibers consist of crystallites with the exact two-dimensional graphite

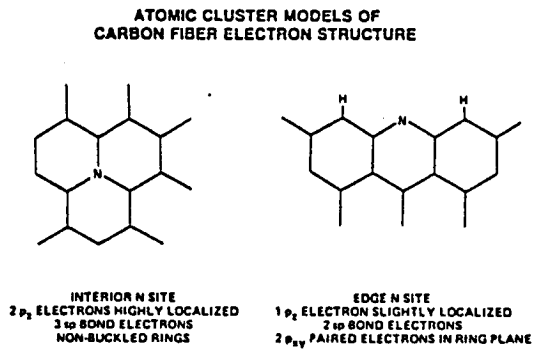

Figure 11 Two different nitrogen locations used for the cluster calculations.

structure, where nitrogen is retained through direct substitutions in the lattice. The resulting model clusters automatically fall into two categories. One can model either an "interior" nitrogen, or an "edge" site, as shown in Fig. 11. Geometry optimization of the clusters yields planar environments for both sites. The edge site, however, has a slightly higher average binding energy. An analysis of the electron distributions of the valence orbital reveals that the edge nitrogen bonding to its carbons is similar to that of an edge carbon-hydrogen pair. However, the interior nitrogen, while maintaining similar bonding on the basal plane, results in rather localized π electron distribution around itself.

To explain these cluster findings in the context of an extended band picture would seem presumptous at best. However, while the band calculations of Rabii [25] are still in progress, we regard for the time being the conclusion of Butkus and Yang on electrical conductivity of PAN carbon fibers as one plausible qualitative explanation.

Based on these results, and the well-known two-dimensinal graphite band structure, Butkus and Yang [24] suggest a flattening of the π bands due to less π delocalization. The consequences, in the somewhat simplified picture of semiconductor band theory, are two fold. First, the effective masses increase, decreasing the carrier mobilities. Second, the π - band flattening inevitably gives rise to a larger band gap, resulting in lower carrier densities. Hence, nitrogen in carbon fibers, especially the interior one, constitutes one physical mechanism by which conductivity is reduced.

4. Conclusions and Discussion

It is clear that we are presently only at the beginning of our understanding of the electronic properties of carbon fibers. We have gained a mass of information of the structural properties of these materials, mainly because of the commercial interest in their use in composites, but we lack a definitive understanding of their basic electronic structure.

Basic to the problem is the lack of crystalline order. In one sense the electronic response to temperature variation is similar to that of a semiconductor, yet on the other hand, we know that increasing conductivity with increasing temperature is also a property of an amorphous material. How can we discern the true nature of these materials?

The attempt here has been to review the basic knowledge of the properties of PAN-based carbon fibers and to couch these properties in the language of simple models. The cluster calculation is the first fundamental theoretical investigation into the nature of PAN-based carbon fibers. We hope that it will shed light for coming investigators. More research is definitely needed.

References

1 C. Héninckx, R. Perret, and W. Ruland, Carbon 10, 711 (1972).

2 F.L. Vogel, Carbon 14, 175 (1976)

3 D.J. Gillsepie, A.C. Ehrlich, and P.F. Waters, Syn. Metals, sumbitted for publication, 1980.

4 I.L. Kalnin and H.A. Goldberg, Syn. Metals, submitted for publication, 1980.

5 See, e.g., G.M. Jenkins and K. Kawamura, Polymeric Carbons (Cambridge University Press, Cambridge, 1976), p. 29 ff.

6 W. Watt, Proc. Roy. Cos. A 319, 5 (1970), and W. Watt, Carbon 10 , 121 (1972)

7 A.K. Fiedler, E. Fitzer, and F. Rozploch, Carbon 11, 426 (1973)

8 W. Watt and W. Johnson, Proc. 3rd International Conference on Industrial Carbons and Graphite, London, 1970, p.417. Also see Ref. 10.

9 B.J. Wicks, J. Nucl. Mater. 56, 287 (1975).

10 W.N. Reynolds, Chemistry and Physics of Carbon, edited by P.L. Walker, Jr. and P.A. Thrower (Marcel Dekker, New York, 1973), Vol. 11, p.1.

11 D.J. Johnson and C.N. Tyson, Brit. J. Appl. Phys. (J. Phys. D) 3, 526, (1970).

12 F.R. Barnet and M.K. Noor, NOLTR 73-154; and, Proc. 2nd Int. Conf. Carbon Fibers, London, 1974 (Plastics Institute, London 1974).

13 S.C. Bennett and D.J. Johnson, Carbon 17, 25 (1979).

14 T. Yamaguchi, Carbon 2, 95 (1964).

15 H.M. Ezekiel, J. Appl. Phys. 41, 5351 (1970).

16 A.A. Bright, and L.S. Singer, Carbon 17, 59 (1979).

17 C. Hefinckx, Carbon 11, 199 (1973).

18 D. Robson, F.Y.I. Assabghy, and D.J.E. Ingram, J. Phys. D 5, 169 (1972).

19 P. Delhaes, P. de Kepper, and M. Uhlrich, Phil, Mag. 29 1301 (1974).

20 A.A. Bright, Carbon 17, 259 (1979).

21 H. Akamatu and H. Inokuchi, J. Chem. Phys. 18, 810 (1950).

22 S. Mrozowski, Carbon 9, 97 (1971).

23 K. Yazawa, J. Phys. Soc. Japan 26, 1407 (1969).

24 A.M. Butkus and C.Y. Yang, Syn. Metals, submitted for publication, 1980.

25 S. Rabii, R.C. Tatar, and D.P. DiVincenzo, Syn. Metals, submitted for publication, 1980.

Appendix III

Cluster Model Studies of Oxygen Intercalated Graphite

Aldona M. Butkus

Surface Analytic Research, Inc.
1662 Parkhills Avenue
Los Altos, CA 94022

Abstract

Electronic structure calculations were carried out on clusters of atoms modeling oxygen intercalation of graphite using the modified intermediate neglect of differential overlap (MINDO) molecular orbital method. The graphite models consisted of both a full three dimensional representation as well as an independent layer model of the lattice. Four different positions for the oxygen atom were considered and consisted of 1) an oxygen directly above a carbon of one layer and directly below that of the second (site A), 2) an oxygen above a carbon of one layer and below the center of a hexagonal ring of the second layer (site B), 3) an oxygen above a carbon-carbon bond and below a position midway between second nearest neighbors of the hexagonal ring (site C), and 4) an oxygen above and below a point midway between second nearest neighbors of the hexagonal rings in both layers (site D). The oxygen-graphite layer distances in the cluster models were optimized within a rigid lattice approximation resulting in the bond site being the most energetically favored position for the oxygen atom at a distance of 1.25Å above the carbon-carbon bond. Additionally, oxygen interaction with the carbons of only one graphite plane predominated not only for the most favored position but for all four sites considered, with the three dimensional results differing little from those obtained using the independent layer model for the various sites.

I. Introduction

Graphite consists of planes of linked hexagons of carbon atoms parallel to one another along the principal C_6 axis. Under certain conditions it is able to take up atoms, ions, or molecules with the lattice structure largely unchanged. These intercalation compounds have been the focus of both experimental and theoretical interest not only for their unusual electronic and chemical properties but also because of their technological possibilities.[1] The work reported here is a theoretical study of the electronic structure of the oxygen graphite system.

The graphite crystal structure is well known, consisting of hexagonal unit cells containing four atoms. The stacking sequence is of ABAB... type where alternate layers are equivalent. Within the layer planes, each carbon atom is surrounded by three other carbons at a distance of 1.42Å. The separation between the layers is 3.35Å and thus clearly indicates that interaction between atoms in adjacent planes is less pronounced than between intra-plane carbons. If in-plane as well as off-plane nearest neighbor atoms are considered, the graphite crystal structure gives rise to two different types of atomic environments. In one type of environment an atom has three in-plane neighbor atoms and carbons directly above and below it in adjacent planes. The other type of atom site does not possess the latter two atoms.

In contrast, little is definitively known about the structure of the oxygen intercalation compounds of graphite. The reported carbon/oxygen ratios are never lower than two and range from 2.4 to 4.0 depending on the degree of oxidation.[2] X-ray studies indicate that the separation of carbon layers falls within the range of

6 - 11 Å.[3] There is some controversy regarding the planarity of the carbon layers since in view of the absence of metallic properties it is believed that the layers would not be planar as in graphite. The carbon atom now attached to four ligands would be tetrahedral causing the layers to buckle. However, more recent electron microscopy and x-ray diffraction studies done by Carr[4] suggest that the layers in oxygen graphite are flat.

For the present cluster model studies of oxygen intercalated graphite, the graphite layers were assumed to be flat and the atoms at their equilibrium positions. Attention was directed toward the determination of the most energetically favored site for the oxygen atom and the elucidation of the type of bonding without any lattice relaxation allowed to take place. Oxygen intercalation in the dilute limit was modeled since interaction between oxygen atoms was not considered.

II. Method of Calculation

The present study of the electronic structure of oxygen intercalated graphite consists of using clusters of carbon, hydrogen and oxygen atoms to model the oxygen-graphite system and carrying out modified intermediate neglect of differential overlap (MINDO/3) molecular orbital calculations.[5] This particular molecular orbital approach, though semi-empirical in nature affords the ability to study large molecular models of the graphite lattice with sufficient economy, providing a useful approximation to the solution of the Hartree-Fock equations. The savings in computational requirements is achieved by the replacement of certain difficult integrals by appropriately determined parameters. The particular parameterization

in the MINDO/3 approach relies on the accurate reproduction of experimental geometries and heat of formation of molecules containing the appropriate molecular species.[6]

In choosing the cluster models of the oxygen intercalant sites, preliminary calculations were carried out using the independent layer model of the graphite lattice in order to determine possible oxygen binding sites. Models for the graphite layer ranged from a single ring of six carbon atoms to a condensed four ring system. Hydrogen atoms at a carbon-hydrogen distance of 1.1Å were used to saturate the dangling σ carbon bonds at the edges of the cluster models. Such a treatment of edge carbons was not expected to introduce great error since the oxygen-lattice interaction should mainly take place with the π electron system. Additionally, energy differences between the lattice model and the lattice-oxygen intercalant model were of interest so that cancellation of errors due to the edge treatment was expected to occur. Use of the independent layer model of the lattice further allowed the determination of the minimum cluster size necessary to adequately represent a property of interest. Comparison of the present two dimensional lattice MINDO results with the only theoretical studies of the oxygen-graphite system done previously concerned with chemisorption[7,8,9] was also possible.

Four different positions for the oxygen atom in the graphite lattice were considered and the cluster models chosen for study are indicated in Figures 1,2,3 and 4. The first site, site A, places the oxygen directly above and below carbon atoms. The second, site B, has the oxygen directly above a carbon and below the center of a hexagonal ring of the second layer. Thus in the independent layer models of this site, clusters are considered with the oxygen above a

carbon as well as above the center of a ring of carbons separately. The oxygen can also be positioned above a carbon-carbon bond, site C, which results in a position below a point midway between second nearest neighbors of the second ring in the three dimensional lattice model. The last oxygen-graphite site considered consists of the oxygen above and below the point midway between second nearest neighbors of the hexagonal rings.

For all of the oxygen-graphite sites considered, MINDO calculations were first carried out on the simplest model of the lattice, a single ring of six carbon and six hydrogen atoms, obtaining the equilibrium oxygen to lattice distance. These values were then used for the calculations on the two ring models directly as well as reoptimized. Since the distances, charge distributions, and binding energies did not change significantly between the optimized and non-optimized calculations, the oxygen to lattice distance was not redetermined in the larger structures of the two dimensional lattice models. For the three dimensional lattice models, the oxygen-lattice distance was again allowed to vary. All calculations were done within a rigid lattice approximation. Binding energies for the oxygen atom were determined from the difference between the calculated heats of formation of the oxygen-graphite models, the analogous pure graphite models and the experimental value of 59.559 kcal/mole for the oxygen heat of atomization used in the parameterization procedure of MINDO. Electronic charges on the atoms were calculated using the Mulliken population approach.[10]

III. Results and Discussion

Before the oxygen-graphite calculations were done, the degree to which the various models of the lattice describe a perfect infinite system was checked. Two quantities often used are the valence charge residing on each atom, with a value of 4.00 for the ideal case, and the cohesive energy of the lattice, the negative of the binding energy with an experimental value of approximately 5 eV/atom.[11] This latter quantity is of particular interest since the previous theoretical studies of oxygen chemisorption on graphite resulted in an overestimation of the lattice energy leading to the prescription of arbitrarily dividing the binding energies by a factor of 5.

The various clusters chosen to model a single layer of the graphite lattice together with the calculated average binding energy per atom and the valence charge are presented in figure 5. For the three dimensional graphite models with an inter-layer spacing of 3.35Å, the valence charge did not differ from the analogous two models. The good agreement between the calculated valence charges for the lattice models and the ideal graphite value indicates that with proper treatment of edge atoms even small clusters can adequately simulate the extended lattice.

For the oxygen graphite models, results consisting of the atomic charges and oxygen binding energies at indicated oxygen to lattice distances are summarized in Tables I, II, and III. The most stable position for the oxygen atom is predicted to be above a carbon-carbon bond at a distance of 1.25Å for both the independent layer and the three dimensional lattice models. The oxygen atom is negative by almost half of an electron with the nearest carbons in the plane

becoming positive. Comparison of the results for the various models of this oxygen-graphite site in Table III, the oxygen-lattice distances and charge distributions do not change significantly from the poorest model (VIII) where the oxygen is above an edge bond to the best model (X) where there are at least two shells of outer carbons about the bonding site. The local nature of this oxygen interaction with the nearest two carbons is thus evident. The carbon-oxygen distance and charge distributions are typical of those found in epoxide molecules.

Considering the next favored position consisting of an oxygen above a carbon atom, in the three dimensional lattice model this position gives rise to two sites as described previously. For site A where the oxygen is above and below a carbon atom comparison of the calculations with the oxygen at the single plane optimized oxygen to lattice distance and at the point midway between the two lattice layers indicates that the charge on the oxygen (-0.60 electron) does not differ significantly from the single plane results. However, consideration of the overall charge distribution summarized in Table I major differences between the two and three dimensional lattice models arise.

With the single layer models, the oxygen charge is at the expense of the carbon directly below the oxygen as well as those atoms adjacent to this carbon. The presence of the second carbon layer in the three dimensional model allows for the charge on the oxygen to come from carbons on both layers leading to changes only at centers directly bonded to the oxygen and the stabilization of the larger oxygen to lattice distance of 1.67Å. For the single layer case, the smaller oxygen lattice distance of 1.44Å is favored.

Analogous carbon oxygen interactions found in molecules are the ether compounds with carbon oxygen distances of 1.4 - 1.5 Å and carbonyls, carbon oxygen distances of 1.2Å.

For the alternate site, site B, where the oxygen is located above one carbon and below the center of the hexagonal ring of carbons results indicate a less favored position over that of site A. The destabilizing effect of the oxygen unable to interact with the ring atom charge distribution to satisfy bonding requirements is evidenced by the positive oxygen to lattice binding energy for the three dimensional model (VII) and the two dimensional model (VI).

Calculations done on models of the remaining oxygen site studied, site D, again result in a negative oxygen at the expense of the nearest carbon atoms. For the three dimensional model, unlike the site A case, placement of the oxygen at the midpoint between the lattice layers does not result in a lowering of the energy but rather an increase indicating a preferred interaction with only a single graphite layer. This is further supported by the drastic lowering of energy when a bond site position is now made accessible to the oxygen from the upper plane as in the cluster XIV.

Results of the present single lattice calculations compare favorably with the three previous theoretical treatments of the oxygen graphite system even though different clusters were treated as well as the more approximate CNDO semi-empirical molecular orbital method was used. The main difference in the three previous calculations were in the approaches used to model the extended lattice. Bennett, McCarroll and Messmer[7] simulated the perfect layer by imposing periodic boundary connections to limited clusters of carbon atoms. Dovesi, et al[8] used a tight-binding crystalline

orbital approach to study periodic overlayers of atomic oxygen on graphite. The work of Hayns[9] most closely paralleled the cluster approach for the two dimensional lattice models presented here in that hydrogen atoms were used to saturate the dangling bonds at the edges of similar clusters. All three calculations were in agreement with the present results showing the bond site to be most stable followed by the atom site. Direct comparison of energies was not possible since it is well known that the CNDO approximation consistently overestimates the binding energy. Additionally, in the MINDO approximation parameters had been adjusted to give the best fit to experimental enthalpies at 298 °K and hence would somehow incorporate macroscopic dynamical effects into a static molecular calculation. The closer agreement to the experimental value of the lattice cohesive energy using the MINDO approximation compared with the CNDO approach may be due to this parameterization. The choice of parameters could also explain the discrepency between the present results and the calculations of Hayns corresponding to a system at 0 °K predicting oxygen binding at the site D position in contrast to the present results. Comparison of the present calculations with the previous theoretical treatments is summarized in Tables V and VI.

Thus from the calculations done on cluster models of oxygen intercalated graphite using the semi-empirical MINDO/3 molecular orbital approach predictions of oxygen binding locations, charge transfers and relative strengths of bindings have been made. Future work on this system would need to consider possible interaction between oxygen atoms corresponding to a less dilute intercalation case as well as to allow changes in lattice geometry. An encouraging

aspect of the present study is the apparent ability to model the extended lattice using finite clusters once care has been taken to adequately saturate the bonding on the edge atoms. Though the present results are at best semi-quantitative in nature, they do offer information not yet available from experimental data.

Acknowledgements

This work is supported by the National Aeronautics and Space Administration Ames Research Center under Contract NAS2-10188.

References

1. J.E. Fischer and T.E. Thompson, Phys. Today, 31, 36 (1978).

2. W. Rudorff, Prog. Inorg. Chem. and Radio. Chem., 1, 223 (1959).

3. G.H. Hennig, Prog. Inorg. Chem., 1, 125 (1959).

4. K. E. Carr, Carbon 8, 155 (1970); 8, 245 (1970).

5. MINDO/3 program from National Resource for Computational Chemistry, Lawrence Berkeley Laboratory, Berkeley, CA.

6. R.C. Bingham, M.J.S. Dewar, and D.H. Lo, J. Amer. Chem. Soc., 97, 1285 (1975).

7. A.J. Bennett, B. McCarroll, and R.P. Messmer, Phys. Rev.B, 3,1397 (1971).

8. R. Dovesi, C. Pisani, F. Ricca, and C. Roetti, Surface Science, 75, 316 (1978).

9. M.R. Hayns, Theoret. Chim. Acta, 39, 61 (1975).

10. R. S. Mulliken, J. Chem. Phys., 23, 1833 (1955).

11. M. Kanter, Phys. Rev. 107, 655 (1955).

Table I. Calculated atomic charges for cluster models of the oxygen-graphite system, site A. Carbon numbering sequence refers to Figure 1. For the three dimensional lattice model, the oxygen-lattice distance, D, refers to the lower lattice plane. Oxygen binding energy, E, is given in eV.

	I	II		III	IV	
O	-0.5951	-0.5971	-0.5921	-0.6222	-0.6042	-0.5988
C_1	0.2402	0.2314	0.2189	0.2127	0.2250	0.1734
C_2	0.2273	0.1644	0.1617	0.2336	0.1358	0.0820
C_3	-0.1463	-0.1325	-0.1256	-0.1018	-0.1115	-0.0574
C_4	0.1874	0.1669	0.1620	0.0978	0.1281	0.0655
C_5	-0.1463	-0.1560	-0.1495	-0.0481	-0.1288	-0.0731
C_6	0.2273	0.2602	0.2556	0.1422	0.2111	0.1351
C_7					0.1148	0.1455
C_8					0.0566	0.1262
C_9					-0.0216	-0.0647
C_{10}					0.0296	0.0881
D(Å)	1.4139[a]	1.4139	1.4436[a]	1.4139	1.4436	1.6750
E(eV)	-0.587	-0.139	-0.155	-0.204	-0.163	-0.402

[a]Oxygen-lattice distance optimized.

Table II. Calculated atomic charges for cluster models of the oxygen-graphite system, site B. Carbon numbering sequence refers to Figure 2. For the three dimensional lattice model, the oxygen lattice distance, D, refers to the lower lattice plane. Oxygen binding energy, E, is reported in eV. All oxygen-lattice distances were optimized.

	V	VI	VII
O	-0.5921	-0.6556	-0.5964
C_1	0.2189		0.2254
C_2	0.1617		0.1543
C_3	-0.1256		-0.1252
C_4	0.1620		0.1538
C_5	-0.1495		-0.1474
C_6	0.2556		0.2456
C_7		0.1706	0.0351
C_8		0.1706	0.0357
C_9		0.1706	0.0352
C_{10}		0.1706	0.0338
D(Å)	1.4436	1.0515	1.4212
E(eV)	-0.155	2.132	0.565

Table III. Calculated atomic charges for cluster models of the oxygen-graphite system, site C. Carbon numbering sequence refers to figure 3. For the three dimensional lattice model, the oxygen lattice distance, D, refers to the lower lattice plane. Oxygen binding energy, E, is given in eV.

	VIII	IX		X	XI	
O	-0.4453	-0.4577	-0.4618	-0.4646	-0.4600	-0.4606
C_1	0.2817	0.3063	0.3033	0.2838	0.2993	0.2989
C_2	-0.0450	-0.0638	-0.0620	-0.0161	-0.0653	-0.0651
C_3	0.0190	0.0206	0.0212	-0.0025	0.0207	0.0208
C_4	0.0190	0.0206	0.0212	-0.0025	0.0144	0.0144
C_5	-0.0450	-0.0638	-0.0638	-0.0161	-0.0571	-0.0568
C_6	0.2817	0.3063	0.3033	0.2838	0.2875	0.2869
C_7				-0.0007		
C_8				-0.0038		
C_9					0.0537	0.0039
C_{10}					0.0326	0.0031
C_{11}					0.0047	0.0051
C_{12}					0.0090	0.0038
D(Å)	1.2318[a]	1.2318	1.2511[a]	1.2318	1.2511	1.2537[a]
E(eV)	-2.756	-1.774	-1.783	-1.408	-1.336	-1.336

[a]Oxygen-lattice distances optimized.

Table IV. Calculated atomic charges for cluster models of the oxygen-graphite system, site D. Carbon numbering sequence refers to Figure 4. For the three dimensional lattice model, the oxygen lattice distance, D, refers to the lower lattice plane. Oxygen binding energy, E, is reported in eV.

	XII	XIII		XIV
O	-0.5302	-0.5292	-0.5454	-0.5198
C_1	0.2001	0.1972	0.1248	0.1270
C_2	0.3143	0.2913	0.1337	0.1111
C_3	-0.2107	-0.1958	-0.0455	-0.0316
C_4	0.2257	0.1960	0.0694	0.0490
C_5	-0.2107	0.2913	-0.0455	-0.0327
C_6	0.3143	0.1972	0.1337	0.1097
C_7		0.0694	0.1248	0.1932
C_8		0.0412	0.1337	0.1375
C_9		-0.0005	-0.0455	0.0152
C_{10}		0.0128	0.0694	-0.0035
C_{11}		-0.0005	-0.0455	0.0331
C_{12}		0.0412	0.1337	-0.0309
D(Å)	1.2702[a]	1.2702	1.6750	1.6750
E(eV)	-0.336	0.030	0.362	-0.406

[a]Oxygen-lattice distance optimized.

Table V. Comparison of the oxygen atom charge for the oxygen atom above a carbon atom, a carbon-carbon bond, and the center of the hexagonal ring. All results are for single layer models.

Present results:	Atom	Bond	Center
single ring	-0.60	-0.45	-0.66
two rings	-0.60	-0.46	———
four rings	-0.62	-0.47	———
Reference 7	-0.40	-0.25	-0.19
Reference 8	-0.30	-0.25	-0.30

Table VI. Comparison of the oxygen-graphite equilibrium distance for the oxygen atom above a carbon atom, a carbon-carbon bond, and the center of the hexagonal ring. All results are for single layer models.

Present results:	Atom	Bond	Center
single ring	1.41	1.23	1.05
two rings	1.44	1.25	——
Reference 7	1.50	1.25	1.00
Reference 8	1.45	1.20	0.80
Reference 9	——	1.25	——

Figure Captions:

Figure 1. Clusters chosen to model oxygen directly above carbon atom, site A. For the three dimensional lattice model IV the upper graphite layer (C_7, C_8, C_9, C_{10}) is indicated by dashed lines. The oxygen atom is above C_1 in all structures. Hydrogens along the edges have been omitted for clarity.

Figure 2. Clusters modeling oxygen-graphite site B. The oxygen atom is above C_1 in structures V and VII. The upper graphite layer (C_7, C_8, C_9, C_{10}) in structure VII is indicated by dashed lines.

Figure 3. Clusters modeling the bond site position site C. Upper graphite layer (C_9, C_{10}, C_{11}, C_{12}) in structure XI is indicated by dashed lines.

Figure 4. Clusters modeling oxygen position site D. The upper graphite layer (C_7, C_8, C_9, C_{10}, C_{11}, C_{12}) in structure XIII and XIV is indicated by dashed lines with the oxygen atom located between the two layers.

Figure 5. Clusters modeling the graphite lattice with the calculated valence charge indicated. Binding energies are reported for each structure in units of eV/atom enclosed in parenthesis.

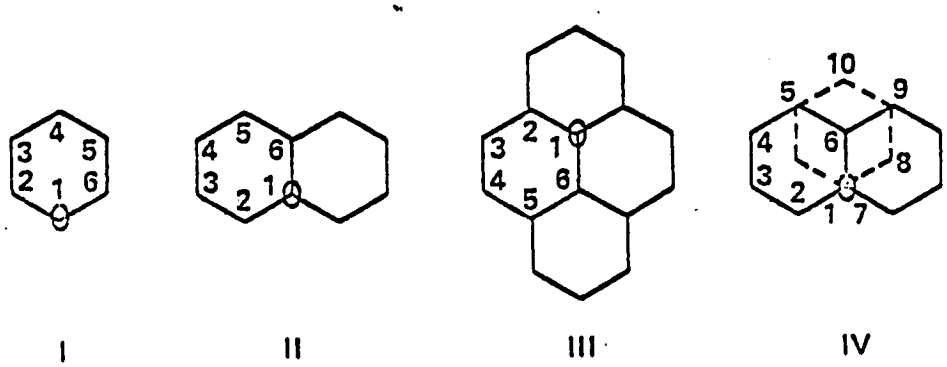

Figure 1

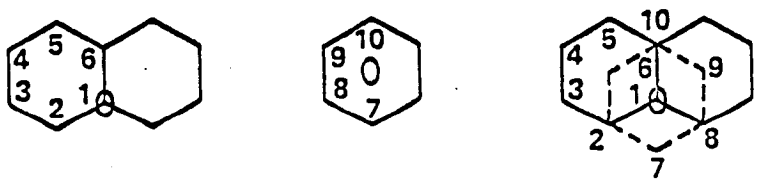

V VI VII

Figure 2

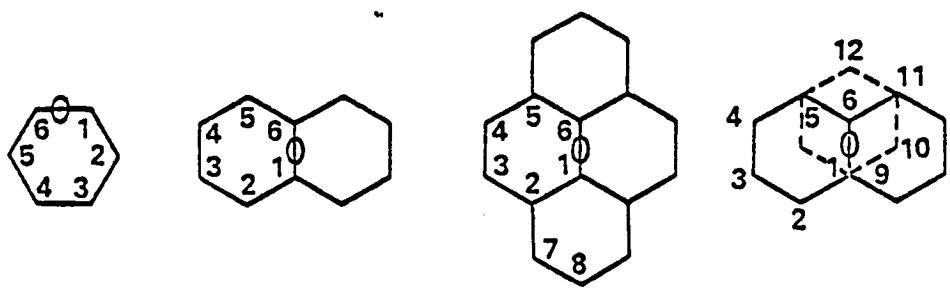

Figure 3

XII

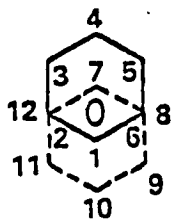

XIII

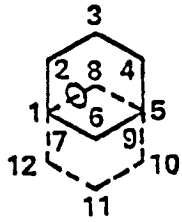

XIV

Figure 4

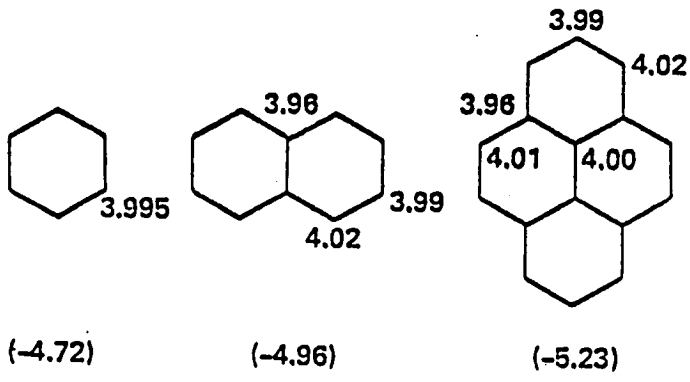

Figure 5

1. Report No.	2. Government Accession No.	3. Recipient's Catalog No.
4. Title and Subtitle CARBON FIBERS CONDUCTIVITY STUDY		5. Report Date August 1980 6. Performing Organization Code
7. Author(s) Cary Y. Yang and Aldona M. Butkus		8. Performing Organization Report No.
9. Performing Organization Name and Address Surface Analytic Research, Inc. 1662 Parkhills Avenue Los Altos, CA 94022		10. Work Unit No. T-4227 11. Contract or Grant No. NAS2-10188
12. Sponsoring Agency Name and Address National Aeronautics and Space Administration Washington, D. C. 20546		13. Type of Report and Period Covered Contractor Report Final Report 14. Sponsoring Agency Code 506-53-11

15. Supplementary Notes

Ames Technical Monitor - James O. Arnold, Mail Stop 230-3, Moffett Field CA 94035
(415) 965-6209 FTS: 448-6209

16. Abstract

In an attempt to understand the process of electrical conduction in polyacrylonitrile (PAN)-based carbon fibers, calculations were carried out on cluster models of the fiber consisting of carbon, nitrogen and hydrogen atoms using the modified intermediate neglect of differential overlap (MINDO) molecular orbital (MO) method. The models were developed based on the assumption that PAN carbon fibers obtained with heat treatment temperatures (HTT) below 1000°C retain nitrogen in a graphite-like lattice. For clusters modeling an "edge" nitrogen site, analysis of the occupied MO's indicated an electron distribution similar to that of graphite. A similar analysis for the somewhat less stable "interior" nitrogen site revealed a partially localized π electron distribution around the nitrogen atom. The differences in bonding trends and structural stability between edge and interior nitrogen clusters led to a two-step process proposed for nitrogen evolution with increasing HTT.

17. Key Words (Suggested by Author(s))	18. Distribution Statement
Carbon fibers, conductivity Electronic structure Pan carbon fibers	Unclassified - Unlimited STAR Category 24

19. Security Classif. (of this report)	20. Security Classif. (of this page)	21. No. of Pages	22. Price*
Unclassified	Unclassified	77	

*For sale by the National Technical Information Service, Springfield, Virginia 22161

End of Document